Water Air Soil Pollut (2019) 230: 180
https://doi.org/10.1007/s11270-019-4226-6

Wet Dust Sampler—a Sampling Method for Road Dust Quantification and Analyses

Joacim Lundberg · Göran Blomqvist · Mats Gustafsson · Sara Janhäll · Ida Järlskog

Received: 14 March 2019 / Accepted: 8 July 2019 / Published online: 24 July 2019

Abstract In northern countries, the climate, and consequently the use of studded tyres and winter traction sanding, causes accumulation of road dust over winter and spring, resulting in high PM_{10} concentrations during springtime dusting events. To quantify the dust at the road surface, a method—the wet dust sampler (WDS)—was developed allowing repeatable sampling also under wet and snowy conditions. The principle of operation is flushing high-pressurised water over a defined surface area and transferring the dust laden water into a container for further analyses. The WDS has been used for some time and is presented in detail to the international scientific community as reported by Jonsson et al. (2008) and Gustafsson et al. (2019), and in this paper, the latest version is presented together with an evaluation of its performance. To evaluate the WDS, the ejected water amount was measured, as well as water losses in different parts of the sampling system, together with indicative dust measurement using turbidity as a proxy for dust concentration. The results show that the WDS, when accounting for all losses, have a predictable and repeatable water performance, with no impact on performance based on the variety of asphalt surface types included in this study, given undamaged surfaces. The largest loss was found to be water retained on the surface, and the dust measurements imply that this might not have as large impact on the sampled dust as could be expected. A theoretical particle mass balance shows small particle losses, while field measurements show higher losses. Several tests are suggested to validate and improve on the mass balances. Finally, the WDS is found to perform well and is able to contribute to further knowledge regarding road dust implications for air pollution.

Keywords Road dust · Sampling · Method · Performance · Road surface

1 Introduction

In urban environments, airborne particles are a major air quality problem related to human health and annoyance (e.g. Forsberg et al. 2005; Meister et al. 2012; Stafoggia et al. 2013; Gustafsson et al. 2014; Shaughnessy et al. 2015; Lanzinger et al. 2016), and the resulting socio-economic impact (e.g. WHO Regional Office for Europe OECD 2015). Research has for long focused on exhaust particles, but since the introduction of electrical cars and low-emission vehicles, the interest is moving towards non-exhaust particles, i.e. abrasion

J. Lundberg (✉) · G. Blomqvist · M. Gustafsson · I. Järlskog
Swedish National Road and Transport Research Institute (VTI), 581 95 Linköping, Sweden
e-mail: joacim.lundberg@vti.se

J. Lundberg
Department of Building Materials, KTH Royal Institute of Technology, Stockholm, Sweden

S. Janhäll
RISE Research Institutes of Sweden, Borås, Sweden

wear from tyres, brakes and roads as well as resuspension of road dust (Gustafsson et al. 2008; Thorpe and Harrison 2008; Gustafsson et al. 2009; Harrison et al. 2012; Grigoratos and Martini 2015; Amato 2018). Still, non-exhaust particle emissions are not regulated even though their effect on human health is non-neglectable (Gustafsson et al. 2008; Denier van der Gon et al. 2012; Amato et al. 2014). Road dust emissions relate both to the road dust depot on the road and to the suspension mechanisms of the road dust. The suspension rate depends on meteorological conditions, traffic, tyre type, road surface properties and mobility of the road dust (e.g. Denby et al. 2013a; Denby et al. 2013b). A complication regarding road dust is the lack of common standards to sample and define road dust further complicates data comparison.

The available methods to quantify the road dust either sample the road dust available at the road surface or the suspension of road dust from induced wind shear or tyre-road interactions. The mobile measurement platforms SNIFFER (Pirjola et al. 2004) and TRAKER (Kuhns et al. 2001) focus on the concentrations of particles in the air behind a rolling wheel (maximum PM_{10}), while the PI-SWERL measures airborne particles (PM_{10}) related to a standardised wind shear (Etyemezian et al. 2007; China and James 2012). Methods that sample the available road dust at the surface include the brushing method used in Brazil ($PM_{2.5}$) (Hetem and Andrade 2016) and the vacuum method used in southern Europe (PM_{10}) (Amato et al. 2013), while AP-42 collect material using brushing and vacuuming adding a model for emission calculation from the data (maximum 75 μm, although only calculate maximum PM_{30}) (EPA 1993a). These methods are categorised and described in Table 1.

All the above-mentioned methods require dry conditions for effective sampling or measurement, and there are no sampling artefacts introduced by using another sampling media affecting the dust properties. On the other hand, the methods using brushes might retain or remove particles otherwise sampled. The sampling procedure used for sampling from the road surface might also induce operator related variability to the data. The late autumn, winters and early spring is usually characterised by wet climate in the southern parts of Sweden, and snowy and icy climate in the northern parts. Therefore, the most common road conditions are moist, wet or snowy.[1] This period also coincides with fast-growing road dust reservoirs due to the use of studded tyres and winter traction sanding, emphasising the importance to be able to follow the dust load development during this period. All sampling of the road dust reservoir also normally imposes safety considerations for the operator(s), including full or partial closure of the studied road segment, thus favouring less time-consuming sampling.

To quantify the total road dust load under both dry and wet road surface conditions, a device called the wet dust sampler (WDS) was developed, utilizing high-pressure washing with a known amount of water of a limited sealed surface in order to collect all dust, with a prototype model ready and in use in 2008 (Jonsson et al. 2008).

The WDS method has been used extensively in national projects for investigations of the temporal and spatial variation of road dust load (Gustafsson et al. 2013; Mats Gustafsson et al. 2014; Gustafsson et al. 2015; Gustafsson et al. 2016; Gustafsson et al. 2017; Gustafsson et al. 2019), evaluation of street cleaning (Gustafsson et al. 2011; Janhäll et al. 2016; Järlskog et al. 2017) and for evaluation of dust binding of paved roads (Gustafsson et al. 2010). The WDS system is currently also used in Norway by the Norwegian Public Roads Administration and in Finland by Nordic Envicon Oy, later by the Finnish Environmental Institute (SYKE), taking the first steps towards a common measurement method to allow for comparable measurements. The initial prototype, described in Jonsson et al. (2008), has been replaced by a generic version with several modifications, impacting on both repeatability and ergonomic aspects. Also, despite the rather extensive use, a thorough presentation of the system's performance is missing. Therefore, this paper has two main purposes. The first purpose is to describe the current WDS system for the broader scientific audience. The second purpose is to answer the following questions regarding its performance:

- Which variability is there concerning sampling water amounts and losses?
- Are there major losses in the system, regarding water and dust?

[1] Personal correspondence with Anna Arvidsson, PhD., winter specialist at the Swedish National Road and Transport Research Institute, 2018-09-07.

Table 1 Categorisation and method description for seven different methods, including the WDS

Method	Type	Largest fraction	Method description	Source for method description
SNIFFER*	Mobile	PM_{10}	•Measure particle concentration behind wheel using commercially available equipment •Calculate emission factor	(Pirjola et al. 2004; Pirjola et al. 2009; Pirjola et al. 2010; Kauhaniemi et al. 2014)
TRAKER*	Mobile	PM_{10}	•Measure particle concentration behind wheel using commercially available equipment •Calculate emission factor	(Etyemezian et al. 2003a; Etyemezian et al. 2003b; Etyemezian et al. 2005; Etyemezian et al. 2006)
AP-42*	Stationary	75 μm	•Collect material from roads using brush and vacuum collection •Uses sieving in laboratory to determine silt fraction •Use AP-42 emission model to calculate emission factor from silt and traffic	(EPA 1993a; EPA 1993b; EPA 2011)
PI-SWERL/Mini PI-SWERL*	Stationary	PM_{10}	•Encapsulated cylinder placed on surface •Rotating disk cause wind shear and suspension of dust •Measure PM in chamber using commercially available equipment	(Etyemezian et al. 2007; China and James 2012)
Brushing method**	Stationary	$PM_{2.5}$	•Collect material from roads using brush •Uses sieving in laboratory to determine sizes •Placed in suspension chamber and scattered using compressed air to obtain a homogenic scatter •Air flow into a virtual impactor with PM_{10} inlet and separation of $PM_{2.5}$ fraction •Deposition of $PM_{2.5}$ on membrane filter	(Hetem and Andrade 2016)
Vacuum method**	Stationary	PM_{10}	•Collection of material from roads using vacuum suction with fitted PM_{10} inlet •Air lead to a deposition chamber •Deposition of PM_{10} on filter	(Amato et al. 2013)
WDS	Stationary	2 mm	•High-pressure water washing of sealed surface •Compressed air to transfer dust laden water into suitable container	(Jonsson et al. 2008); This study

*The method is used to estimate emission factors

**The method can possible be used to estimate emission factors, although not primarily intended for it

2 Description of the Wet Dust Sampler

The WDS system consists of several parts (Fig. 1), including a sampling device, an air compressor, a high-pressure water aggregate, a control box, a computer with in-house developed control software and a main water storage container, fitted with a level sensor.

The sampling device (Fig. 1a) is placed on the surface to be sampled. A small circular sampling area (0.002043 m^2) is sealed by the operator standing on the foot plate, thus pressing a circular cellular rubber ring against the surface. A sample is taken by an automated procedure where a known amount of high-pressure water flushes the sampling area and the water with the dust sample is then transferred to a sampling bottle using filtered compressed air (Fig. 2). Depending on the settings provided by the user, the washing process and the sample transfer process can be varied in time length and overlapping as desired. One sampling procedure is referred to as a "shot" in the following text. Shots can be sampled separately or

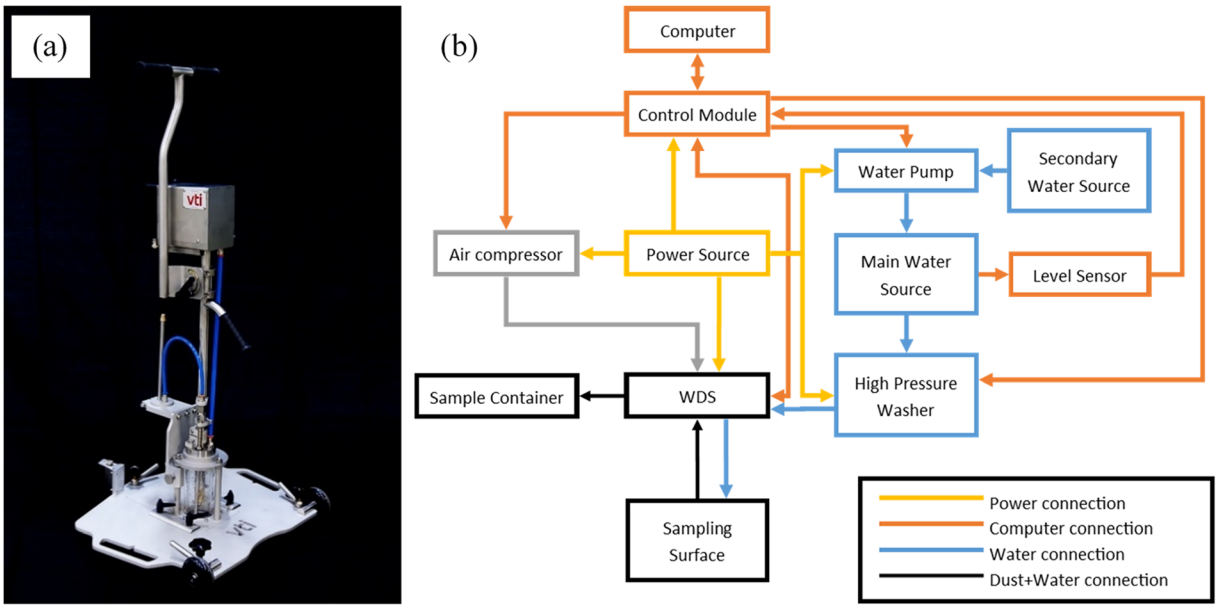

Fig. 1 **a** The wet dust sampler III. Photo: Mats Gustafsson, VTI. **b** Schematic view of the WDS system

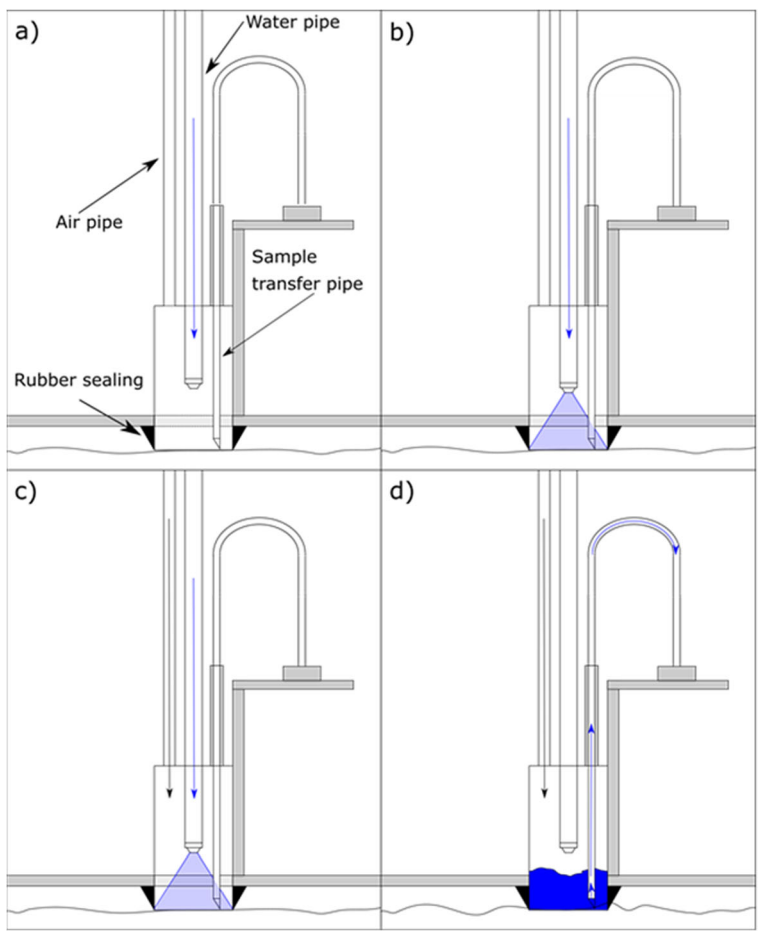

Fig. 2 WDS sampling sequence. While the operator stands on the foot plate, pressing the rubber sealing to the road surface, directly after starting the sampling (i.e. pressing the button), water will be (**a**) transported into the WDS and (**b**) sprayed at high pressure on the surface in a filled conical shape, and thus cleaning it. After given time, (**c**) compressed air is delivered (normally overlapping with the water transport), which starts to (**d**) press the now dust-filled water into the outlet pipe and transferring it from the surface into a suitable container (not showed). This whole process is called a "shot"

be compiled into bigger samples containing several shots. The standard settings used is that water delivery ends after 5 s, while air compression starts at 2 s and ends after 10 s. The sample outlet is spring loaded in order to always be fitted as close to the surface as possible. A schematic drawing of the system is given in Fig. 1b. To be able to sample closer to kerbs, the foot plate can be removed.

Sampling can be performed using different types and qualities of water, depending on what analytical requirements are present. Using de-ionised water have the advantage of enabling analyses of soluble ions, to study the content of salt-based dust binders or de-icers. If the focus of analyses is organic pollutants on the other hand, distilled or other high-quality purified water may be preferred as sampling medium. For all water types, other possible analyses include determining the dust loading, organic content, size distributions and chemical analyses of both insoluble dust and solution as well as morphological particle analyses. A consideration when using the WDS system is the impact of below-zero temperatures risking to freeze water in the system, as well as residual water on the surface, which might be a traffic safety risk. These risks can be lowered, and possibly avoided by using heated water, by removing the residual water or by application of de-icing material on the surface after sampling. Also, as with all methods requiring labour on roads, partial or full closure for traffic is required for the safety of the operators.

In this paper, all field samplings were performed using de-ionised water to be able to follow the use of de-icing and dust binding agents. For the laboratory results, all tests were performed using tap water. The settings used for all tests, both field and laboratory, are the standard settings described above.

3 Evaluation of System Performance

The system performance depends on the road surface macro texture, the dust properties and the level of attachment between the dust and the road. The WDS is thus tested to understand if there is dust left on the surface after sampling, which allows the loss to be accounted for when determining the dust load.

In this paper, a mass balance for the water is performed, followed by a mass balance for the road dust, where a discussion on the amount of road dust available for resuspension is added.

The studies are divided into:

1. Using pressure settings to determine delivered water.
2. Water mass balance, measuring:
    a. Collected water from the surface,
    b. Retained water on the surface,
    c. Retained water on the rubber sealing (Fig. 3a),
    d. Leakage of water between sample container and sampler holder (Fig. 3b),
    e. Leakage of water from container air pressure normaliser (APN, Fig. 3c).

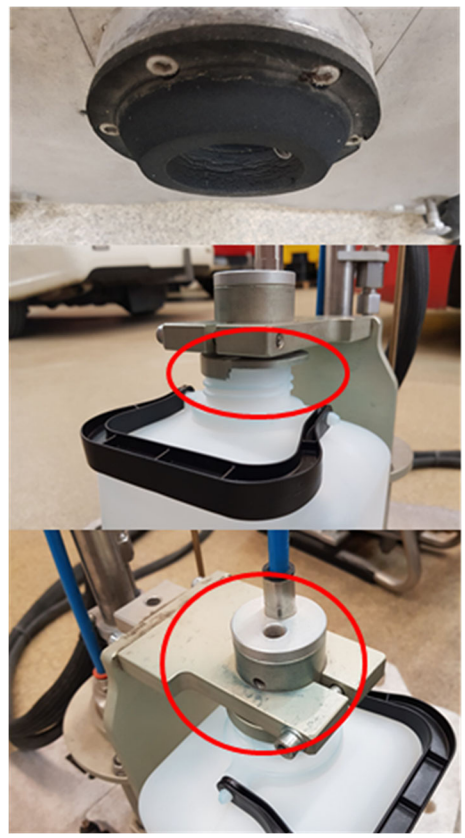

Fig. 3 Locations with potential water losses. **a** The cellular rubber sealing. **b** Area with potential loss between container and WDS holder. **c** Air pressure normaliser, to prevent overpressure in the container. Photos: Joacim Lundberg, VTI

3. Dust mass balance, measuring:
   a. Retention of dust inside the WDS device
   b. Loss of non-collected dust, i.e. dust retained on surface after a sample.
   c. Variation of dust concentration in sample over the sampling time.
4. Theoretical calculation of mass balance.

4 Evaluation of Water Performance

The relation between pressure in the system and delivered water was tested by sampling the ejected water amount directly into pre-weighted bottles. By weighing the bottles with the water, the ejected water mass was calculated. While sampling, the peak pressure shown on the high-pressure water pump was noted for each shot.

In the water mass balance test (2 in the list above):

- (a) were investigated first, sampling from four different surfaces, into pre-weighted containers.
- (b) was performed by using pre-weighted Wettex cloths (absorbent cloth) with which all standing water on the surface was collected. This was done in connection to the sampling in (a). The WDS was moved slightly between each sample. To be noted is that the Wettex method, while being cheap and effective, has some potential drawbacks, such as difficulties absorbing water in deep textures.
- (c) was investigated by performing samples on the earlier described surfaces, after which the WDS was directly placed with the rubber sealing on top of a pre-weighed Wettex cloth, and then loaded by stepping up on the foot plate.
- (d) was investigated by using pre-weighed Wettex cloth, which were placed around the sampling container and container holder to absorb the otherwise leaking water.
- (e) was investigated in a similar manner as point (d), with the difference that the air pressure normaliser was covered by a pre-weighed Wettex cloth.

5 Surface Characterisation

An important way to determine how the surface impacts on the performance is by investigating its surface texture. Macro texture has been shown to affect non-exhaust traffic emissions from the road surface and tyre interaction through the possibility to store dust for later suspension/resuspension, both the volume of the voids in the texture and the morphology of the voids is of importance (e.g. China and James 2012; Blomqvist et al. 2014; Lundberg et al. 2017; Padoan et al. 2018).

In all cases for the laboratory measurements of water performance, the road surface macro texture was determined through the use of the mean texture depth (MTD) (CEN 2010). The MTD is measured using a volumetric method, known as the sand patch method (see CEN 2010). In the dust performance study, mean profile depth (MPD) was used to describe the macro texture of pavement slabs. MPD is a non-contact laser method to determine macro texture profile depth (ISO 13473-1 1997), compared to the volumetric method described earlier. According to the ISO standard, MPD can be recalculated into an estimated texture depth (ETD), which is close to the corresponding MTD values (ISO 13473-1 1997), also expressed in millimeters.

For the laboratory investigation of water behaviour, four different surfaces were selected, described in Table 2. Neither MTD nor MPD give the variation of the texture within the measured area or profile segment, why the surface characteristics are further described by photographs from a 3D-camera (GoCator model 3210 from LMI Technologies Inc.) and a regular camera (Fig. 4).

In the dust performance tests, three different surface types (SMA 11, SMA 8 and SMA 6, *not the same as for water behaviour studies*), with different mean profile depths (MPD, 1.51 mm, 1.06 mm and 0.99 mm respectively) were used. This change of surfaces was due to

Table 2 Surface characteristics for four different surfaces. *SMA*, stone mastic asphalt

Surface type	MTD [mm]
SMA 16	1.00
SMA 8a	1.95
SMA 8b	1.86
Floor (concrete)	0.00*

*Estimated value, not measured

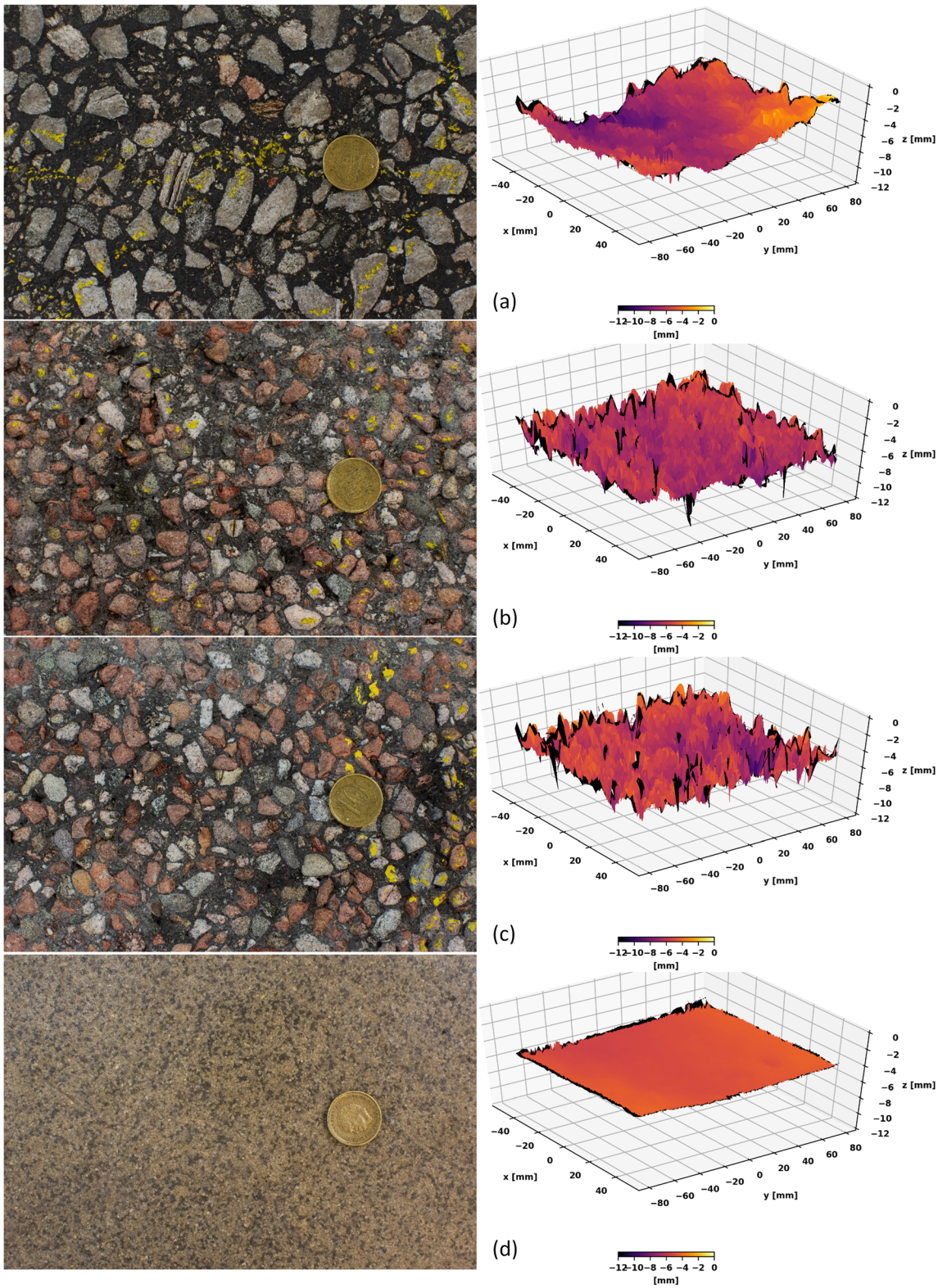

Fig. 4 **a**–**d** Photographs and 3D images (mm-scale) of SMA 16, SMA 8a, SMA 8b, and the floor respectively. The coin has a diameter of 20.5 mm. Photos: Joacim Lundberg, VTI

availability issues for the earlier used types. These were recalculated according to ISO 13473-1 (1997) to the ETD values of 1.41 mm, 1.04 mm and 0.99 mm respectively.

5.1 Statistical Analyses

In some cases, where confidence intervals were calculated, the method of empirical (non-parametric) bootstrap was used (e.g. Wehrens et al. 2000), at a significance level of 5%, using 100 000 bootstrap samples. This was done using RStudio, version 1.1.456.

The empirical bootstrap uses an empirical data set, from which a new simulated data set is picked. This is done by resampling the original data set with replacement a given number of times, in this case 100 000 times, from which then estimators of interest can be calculated, in this case the confidence interval.

Thanks to the method used, no assumption is required of the underlaying distribution, making it suitable for these types of measurements where the distribution is unknown.

5.2 Evaluation of Dust Performance

The identified parameters in this paper regarding the implications of dust behaviour were:

1. Retention of dust inside the WDS system.
2. Loss of non-collected dust, i.e. dust retained on surface after a sample.
3. Variation of dust concentration in sample over the sampling time.

(1) was investigated during field measurements for 12 different street locations, divided between six different streets in central Stockholm, Sweden. After a standard sample (i.e. 6 "shots" into a 2.5-l container) an extra "shot" was taken on top of a clean, flat surface (with no macro texture) into a separate container, thus flushing the system with clean de-ionised water.

(2) was investigated in laboratory environment as well as in field. For the laboratory investigation, the road surface texture was filled with a granite filler dust (570–1780 g/m^2) commonly used in road pavement mixtures, with a density of 2640 kg/m^3, a maximum particle size of 1000 μm, of which about 20% is 10 μm or smaller. Three shots were taken without moving the WDS between the shots. Similar samplings were made under field conditions in Stockholm for 12 different street locations.

(3) was investigated using semi-field environment, i.e. on an actual outdoor pavement surface exposed to weather effects, although not exposed to a realistic traffic situation. The test was made by manually switching sampling bottles in a sequence during the sampling time, with about 1 s water collection per bottle.

For all tests, turbidity was used as a proxy of the dust concentration, even though the result might be affected by particle size distribution and particle properties including light absorption properties, light scattering properties, colour and shape. Turbidity is an optical method utilizing the light scattered by particles when suspended in water and thus estimates the particle concentration (Pavanelli and Bigi 2005). Turbidity is used, e.g. for monitoring of suspendible solids in water (e.g. Grayson et al. 1996; Slaets et al. 2014; Tananaev and Debolskiy 2014). In this paper, all analyses were performed using a HI88713 ISO Turbidity Meter from Hanna Instruments using the formazin nephelometric unit (FNU). The instrument can perform readings in the range of 0–1000 FNU ± 2%. Due to the variation of light scattering, a minimum of three readings were performed per sample and the average was calculated and used in the analyses.

6 Results and Discussion

6.1 WDS Water Behaviour

6.1.1 Delivered Water

A strong correlation is present between the average peak pressure and the mean delivered water weight, as presented in Fig. 5. The obtained equation is:

$$W_{del} = 172 \bullet \ln(P) - 455, R^2 = 0.99 \quad (1)$$

where W_{del} is the delivered water [g] and P is the peak pressure [bar]. In the continued evaluation, this equation will be used to calculate the delivered water based on the measured pressure to allow for calculation of the relative losses.

6.1.2 Water Collection and Water Losses

Several investigations were performed in which the water collection efficiency was determined. Also, the

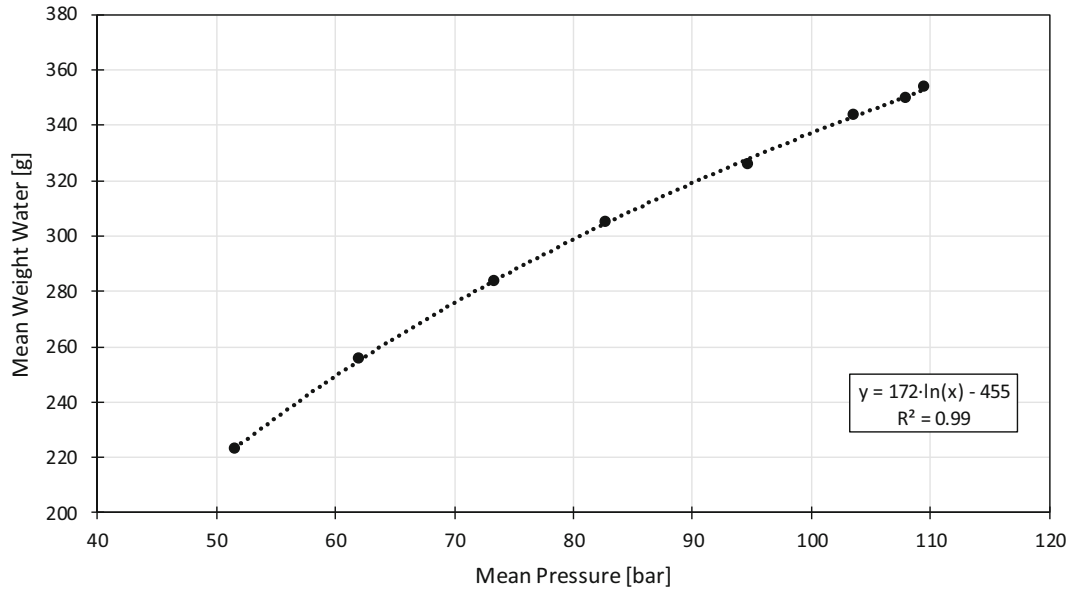

Fig. 5 The relationship between the average peak pressure and the mean flushed water mass. Each of the points is based on 20 measurements (20 "shots"). Standard deviation varies between 0.3 and – 2.4 g for the flushed water

potential sources of losses were quantified. Using Eq. 1, the delivered water was calculated based on the measured peak pressure for the tests.

Figure 6 presents the results for both the calculated delivered water and the collected water, as well as the potential losses, for the four different surfaces investigated. Table 3 presents the calculated confidence intervals.

Looking at the confidence intervals, a few observations can be made:

- There are no significant differences regarding *collected water* between the different asphalt surfaces, but there is a significant difference between the floor and the asphalt surfaces.
- There are no significant differences regarding *surface retained water* between the asphalt surfaces, but there is a significant difference between the floor and the asphalt surfaces.
- The rubber sealing shows more variation, where no clear significance is found between the asphalt surfaces and the floor.

In general, it is surprising that the collected water and the retained water on the asphalt surfaces only showed significant differences compared to the floor surface. This observation indicates that going from entirely smooth texture to a surface texture with MTD = 1 mm will have an impact on the water losses, thus also indicating that particles can be lost. It also shows that increasing the texture roughness (in this case, a maximum MTD of 1.94 mm) will not significantly change the collected amount of water compared to MTD = 1 mm, and thus implying that the loss of particles will not be affected. This is, of course, given the assumption that no leakage, in which the sample is partly lost, occurs between the rubber sealing and the surface. A possible explanation to this difference could be that, on the pavement surfaces, the remaining water at the end of the sampling sequence is hindered by protruding aggregates on its way to the outlet, which is placed on the side of the sampling cylinder.

The loss of water due to absorption or adhesion of water to the cellular rubber sealing shows more variation between the surfaces in terms of significance. This could be linked to the texture roughness, since a rougher texture, even though not causing leakage, might cause more voids between road surface and sealing in which water can intrude and adhere to the sealing surface and thereby be lost from the sample.

The water leakage between the container and WDS, as well as from the air pressure normaliser, shows small losses compared to the delivered water, up to a maximum of 1.5%. For the leakage between the container and the WDS, as well from the air

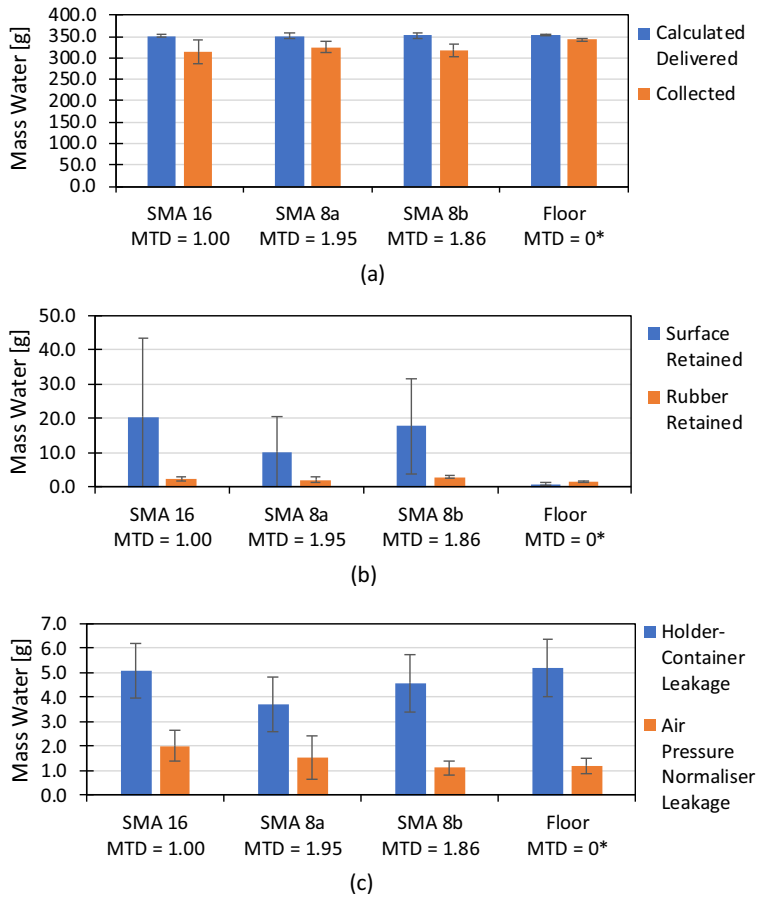

Fig. 6 Variability of water, including standard deviation, for the WDS system for four different surfaces described in Table 4. **a** Comparison of collected and delivered water, where the delivered water is based on peak pressure using Eq. (1). **b** Comparison of water retained on surface and water absorbed or retained on the rubber sealing. **c** Comparison of water leakage between sample container and WDS and the air pressure normaliser. MTD is expressed in milimeters, and * marks an assumed value

pressure normaliser, the levels are somewhat higher than the losses from the cellular rubber sealing, the latter up to a maximum of 0.8%.

Using the total amount of water delivered by the system and the losses described above, the sampled water amount can now be described as:

$$W_{col} = W_{del} - \left(W_{sur} + W_{rub} + W_{con} + W_{apn} + \varepsilon\right) \quad (2)$$

where W_{col} is the collected water [g], W_{del} is the calculated delivered water [g] from Eq. (1), W_{sur} is the water retained on the surface [g], W_{rub} is the water retained by the rubber sealing [g], W_{con} is the water leakage between container and WDS [g], W_{apn} is the leakage from the air pressure normaliser [g], and ε is an unknown error [g], explaining the rest of the losses. Figure 7 illustrates how the sum of the collected water and the different losses, with their proportions, compares to the calculated delivered water.

As can be seen, a major part of the delivered water is collected again by the sampler with rather small losses. The major loss for the asphalt surfaces are in falling order (average, also presented in Table 4): the loss due to surface retention of water (4.6%), the loss due to leakage at the sample container (1.3%), loss due to retention by the rubber sealing (0.7%) and finally the loss due to leakage at the air pressure normaliser (0.4%). For the floor, the largest loss is instead from the leakage between the container and the WDS (1.5%). It can also be seen that no collected water sample reached the calculated delivered water amount (collected water between 89.4 and 96.6% of delivered water), with, in total, less losses for the floor compared to the asphalt surfaces. This is probably due to the surface characteristics, as well as to how well the rubber sealing was able to seal against the surface. The efficiency can also be affected by how high from the lowest parts of the texture the sample outlet is placed during

Table 3 Measured and calculated averages and confidence intervals. Confidence intervals calculated from empirical bootstrap test with 100 000 generated bootstrap samples with $\alpha = 0.05$

	Collected water ($n = 30$)			
	Average [g]	Lower confidence [g]	Upper confidence [g]	Share of delivered water [%]
SMA 16	314.8	305.8	325.1	89.4
SMA 8a	325.6	321.5	330.3	92.6
SMA 8b	317.8	313.1	322.7	90.1
Floor (concrete)	343.3	342.0	344.6	96.6
	Surface retained water ($n = 30$)			
	Average [g]	Lower confidence [g]	Upper confidence [g]	Share of delivered water [%]
SMA 16	20.5	11.9	28.0	5.8
SMA 8a	10.3	6.3	13.6	2.9
SMA 8b	17.7	12.7	22.5	5.0
Floor (concrete)	0.9	0.7	1.0	0.3
	Water retained by rubber sealing ($n = 20$)			
	Average [g]	Lower confidence [g]	Upper confidence [g]	Share of delivered water [%]
SMA 16	2.3	2.0	2.6	0.7
SMA 8a	2.1	1.7	2.4	0.6
SMA 8b	2.8	2.7	3.0	0.8
Floor (concrete)	1.5	1.4	1.7	0.4
	Water leakage sample container and WDS ($n = 20$)			
	Average [g]	Lower confidence [g]	Upper confidence [g]	Share of delivered water [%]
SMA 16	5.1	4.6	5.6	1.4
SMA 8a	3.7	3.2	4.2	1.1
SMA 8b	4.6	4.1	5.1	1.3
Floor (concrete)	5.2	4.7	5.7	1.5
	Water leakage from air pressure normaliser ($n = 20$)			
	Average [g]	Lower confidence [g]	Upper confidence [g]	Share of delivered water [%]
SMA 16	2.0	1.7	2.2	0.6
SMA 8a	1.5	1.1	1.8	0.4
SMA 8b	1.1	1.0	1.2	0.3
Floor (concrete)	1.2	1.1	1.4	0.3
	Calculated delivered water ($n = 30$)			
	Average [g]	Lower confidence [g]	Upper confidence [g]	Share of delivered water [%]
SMA 16	352.1	351.0	353.3	100
SMA 8a	351.5	349.7	354.2	100
SMA 8b	352.9	350.8	355.2	100
Floor (concrete)	355.3	354.7	355.9	100

sampling. In a rough texture, this variation of this position is likely to be higher.

Using the average values presented in Table 4, the share of each parameter in Eq. 2 was summarised, and ε was calculated. As can be seen, the highest unknown error is given by SMA 8b and the lowest unknown error is given by the floor, with SMA 16 and SMA 8a in-between. In general, for the investigated surfaces, 2.5% or less of the calculated delivered water is unknown losses. Possible explanations to unknown losses are not managing to sample the total loss of the other loss categories, loss in other parts of the system, such as the inside of the sample cylinder, losses in transfer tubing and absorption by the sample surface.

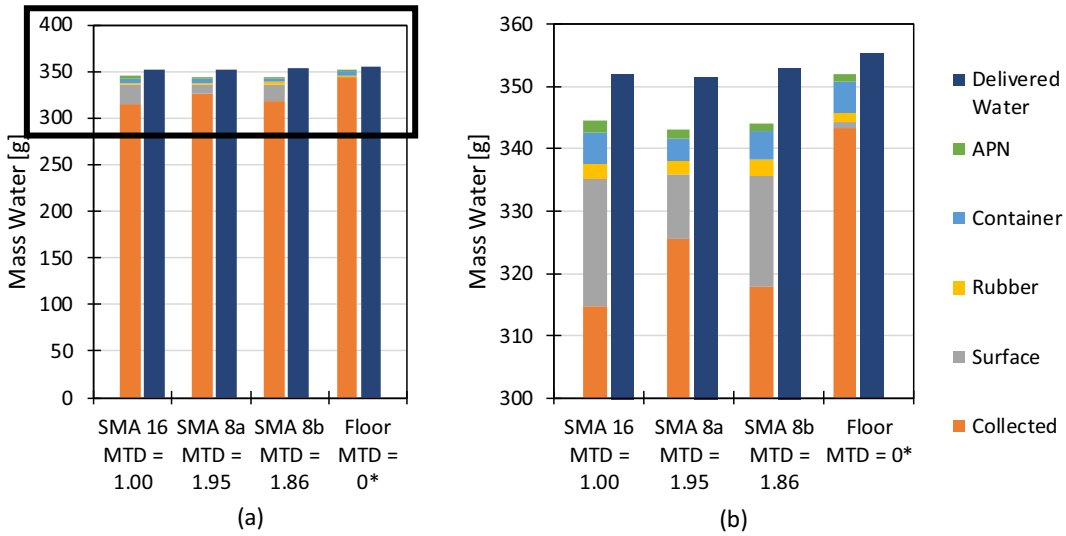

Fig. 7 **a** Illustration of water mass collected and water mass losses with its proportions based on averages in Table 3 and pavement description from Table 2. **b** Magnification of black rectangle in (**a**). MTD is expressed in millimeters, and * marks an assumed value

6.2 Water Mass Balance

By using the data gathered, it is possible to set up a mass balance for the water transport, which can be used to set up a particle balance, as well for deepening the understanding of potential error sources and their magnitude.

This balance, given sampling on the same surface without moving the WDS, can be described in the following way:

$$\begin{aligned}
&\text{Sampling 1}: W_{del,1} = W_{col,1} + W_{con,1} + W_{apn,1} + W_{sur,1} + W_{rub,1} + \varepsilon_1 \\
&\text{Sampling 2}: W_{del,2} + W_{sur,1} + W_{rub,1} + \varepsilon_1 = W_{col,2} + W_{con,2} + W_{apn,2} + W_{sur,2} + W_{rub,2} + \varepsilon_2 \\
&\text{Sampling 3}: W_{del,3} + W_{sur,2} + W_{rub,2} + \varepsilon_2 = W_{col,3} + W_{con,3} + W_{apn,3} + W_{sur,3} + W_{rub,3} + \varepsilon_2 \\
&\text{Sampling n}: W_{del,n} + W_{sur,n} + W_{rub,n-1} + \varepsilon_{n-1} = W_{col,n} + W_{con,n} + W_{apn,n} + W_{sur,n} + W_{rub,n} + \varepsilon_n
\end{aligned} \tag{3}$$

Table 4 Overview of the unknown error based on the measured average values

Surface	Unit	W_{del}	W_{col}	W_{sur}	W_{rub}	W_{con}	W_{apn}	ε
SMA 16	[g]	352.1	314.8	20.5	2.3	5.1	2.0	7.4
	[%]	100	89.4	5.8	0.7	1.4	0.6	2.1
SMA 8a	[g]	351.5	325.6	10.2	2.1	3.7	1.5	8.4
	[%]	100	92.6	2.9	0.6	1.1	0.4	2.4
SMA 8b	[g]	352.9	317.8	17.7	2.8	4.6	1.1	8.8
	[%]	100	90.1	5.0	0.8	1.3	0.3	2.5
Floor	[g]	355.3	343.3	0.9	1.5	5.2	1.2	3.2
	[%]	100	96.6	0.2	0.4	1.5	0.3	0.9
Average*	[g]	352.2	319.4	16.2	2.4	4.5	1.5	8.2
	[%]	100	90.7	4.6	0.7	1.3	0.4	2.3

*Average is calculated based on only the three asphalt surfaces

Given the assumption that:

$$\begin{aligned} W_{sur,k} &= W_{sur,k+1} \\ W_{rub,k} &= W_{rub,k+1} \\ W_{del,k} &= W_{del,k+1} \\ \varepsilon_k &= \varepsilon_{k+1} \end{aligned} \quad (4)$$

With the average values collected from Table 5, sampling 2 and onwards will involve 379 g (26.8 g extra) water delivered or already present on the surface or rubber sealing (combination of present and previous sampling), while only 352.2 g water will be collected or lost in the present sampling only. This difference of 26.8 g water has two possibilities to be explained. Either it is collected, thus increasing W_{col}, or it is lost, increasing the sum of $W_{con} + W_{apn}$, or a combination of both.

To investigate if the assumptions are valid, a test was done for which the four previously described road pavement and floor surfaces were used. On each surface, five samplings were performed on the same sampling area, while not moving the WDS sampling unit. The collected water mass was measured and is presented in Table 5, as well as in Fig. 8.

Using the earlier described method of the empirical bootstrap test with 100 000 generated samples, a 95% confidence interval was calculated for the average water masses for the asphalt surfaces. As can be seen by the results in Table 5, a significance is seen for the difference of 9.6 g between the first sample mass and the repetition sample masses. This implies that at least part of the excess water mass is collected in the next sample. The 17.2 g left (26.8 g extra water in shot 2 and onward, subtracted the 9.6 g difference) is likely then appearing as leakage and thus increase the sum of $W_{con} + W_{apn}$.

6.3 Implications on Dust Losses

6.3.1 Particle Sampling Efficiency

The results from the controlled laboratory studies are given in Fig. 9, while those from the field studies are given in Fig. 10. The laboratory investigation shows that the particle sampling efficiency is high for the three different types of pavements investigated (SMA 11, SMA 8 and SMA 6), not to be confused with those used for the water behaviour studies. In this investigation, the texture was filled with a mineral dust (570–1780 g/m^2) commonly used as filler in pavement mixing designs. The first repetition shows less than 10% of the turbidity in comparison to the first sample, implying a similar percentage of the original dust amount remaining on the surface after the first sampling. The same reasoning applies to the second repetition. The water retained on the surface holds a small amount of remaining dust, which is collected in the repeated samplings, further diluting the dust concentration in the retained water.

For the field studies (Fig. 10), most street locations show similar behaviour as the lab studies, although at different levels. The first repetition samples between 6 and 20% of the amount of the first sample, when not considering location 1, 2 and 6. In these locations, the first repetition instead results in 39%, 77% and 60% respectively, of the amount of the first sample. A possible explanation is differences in sampled dust properties. The dust used in the lab measurements was a homogeneous granite dust, which was applied dry. Field sampled road dust was taken during the Swedish winter period and is heterogeneous, consisting of pavement, tyre and brake wear particles mixed with deposited dust from

Table 5 Measured and calculated average values of collected water weight used for determination of the mass balance assumption. Confidence intervals calculated from empirical bootstrap test with 100 000 generated bootstrap samples with $\alpha = 0.05$

Sample [−]	SMA 16 [g]	SMA 8a [g]	SMA 8b [g]	Floor [g]	Average* [g]	Lower confidence* [g]	Upper confidence* [g]
1	337.5	340.1	318.4	343.5	332.0	324.8	339.2
2	343.9	345.6	334.2	346.5	341.6**	339.6**	343.8**
3	344.1	345.3	333.8	349.3			
4	343.2	345.1	336.4	346.9			
5	344.9	345.1	337.7	347.2			

*Calculated only for the three asphalt surfaces

**Calculated from the average of sample 2-5

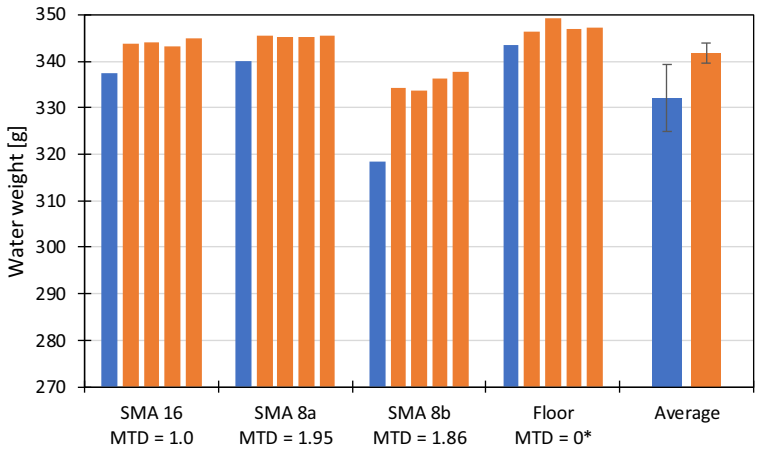

Fig. 8 Illustration on how the first sample (one "shot") and the subsequent repetitions differentiate on the same surface without moving the WDS, as well as the averages for the asphalt surfaces. Observe that the black bars are in this case the 95% confidence interval as described by Table 5. The average and the confidence interval is calculated for the three asphalt surfaces only. MTD is expressed in millimeters, and * marks an assumed value

other nearby and distant sources. This dust is exposed to drying and wetting cycles, traffic and road operation, affecting the properties of the dust as well as dust load compaction and cementation compared to the lab measurements. Cemented dust will be harder to remove from the road surface texture. Differences in texture characteristics might also affect the efficiency, especially cementation in coarser textures, or deeper voids, might prevent dust from being sampled. Other possibly influencing parameters are dust colour and particle size and shape. Field samples are usually darker than the granite dust used in laboratory, which could affect the turbidity measurements. The difference seen, although requiring more research, gives some idea on how the traffic and metrological processes and the surface properties impacts on the dust loading and its ability to be transported.

6.3.2 Dust Retention in System

The result of retention of dust in the system is given in Fig. 11. Possible causes for retention are dust sticking to the inside of transfer tubing or trapped in joints.

For four of the cases presented, turbidity is markedly higher compared to the other samples, but all are still very low compared to the normal measurements performed at the same time, which at the time varies between 13 and 275 FNU. The retention for all cases presented is limited to a minimum of about 6% and 4% for wheel tracks and between wheel tracks respectively. It can be noted that normal turbidity values for these streets during the dusty season vary between 100 and 800 FNU. These results show that the possible retention is likely to be neglectable. The lowest turbidity is from samplings in wheel tracks, while the higher values are from samplings in-between wheel tracks.

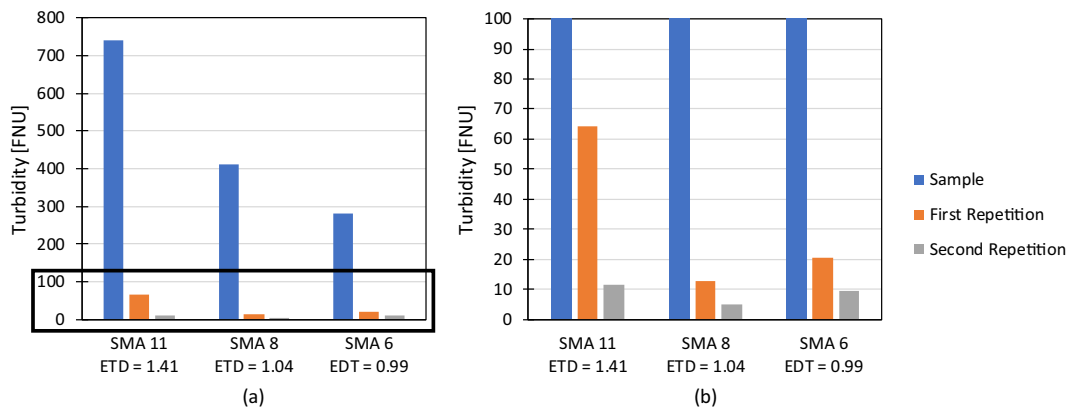

Fig. 9 **a** Particle sampling efficiency for three different asphalt surfaces sustained to abrasion wear in a lab environment using stone dust, expressed as turbidity used as proxy for particle concentration. **b** Magnification of black rectangle in (**a**). ETD is expressed in millimeters

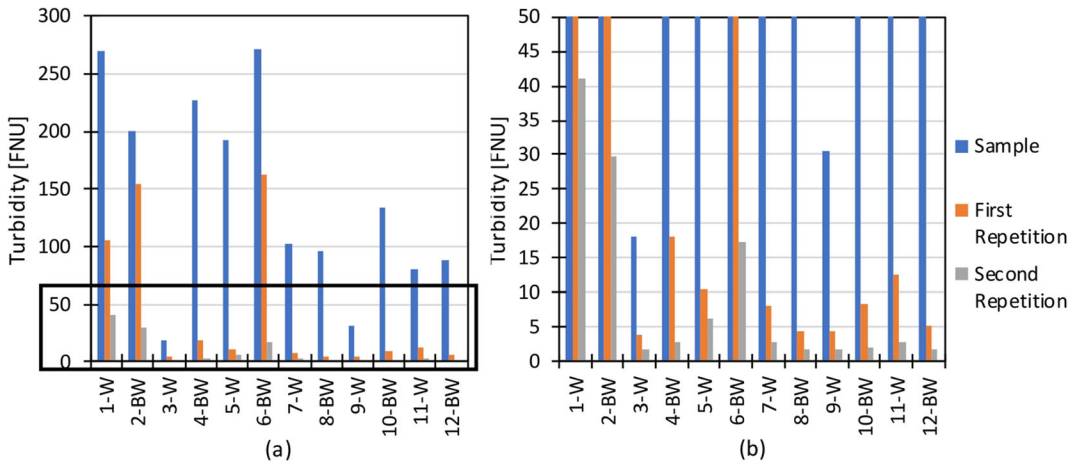

Fig. 10 **a** Particle sampling efficiency for 12 different street locations in Stockholm, Sweden, expressed as turbidity used as proxy for particle concentration. **b** Magnification of the black rectangle in (**a**). W and BW stands for wheel track and between wheel track

The difference is likely to depend on the normally lower dust load in wheel tracks, due to higher suspension forces. Other influencing factors are the dust's inherent properties and meteorology, both over time and at the time of sampling. Further investigations are required to specify the causes for differences in more detail.

6.3.3 Dust Concentration Variability over Sampling Time

Figure 12 displays how turbidity in a sample varies over time during sampling (one "shot"), given current settings for two different road pavement surfaces. Surface 1 is an asphalt surface that are exposed to weather, but not to traffic. Surface 2 is a street location with low traffic amounts in Gothenburg, Sweden. As can be seen, the concentration varies over time for both locations, and the pattern is repeated for all samples, although at different levels. Turbidity is affected by dust load and dust particle properties such as colour, solubility, size and shape. The decreasing trend in turbidity during the sampling is a result of the successively smaller dust load on the surface. The small increase in bottle 4 can be explained by the different phases in the washing process. With the given settings, the washing will gradually increase the water level before the compressed air starts to press out the sample. The spray nozzle will start to wash the surface and simultaneously increase the water level before compressed air starts to press the sample to the sample container. The water flow is very turbulent during this phase. The washing effect will initially decrease due to material being removed and due to

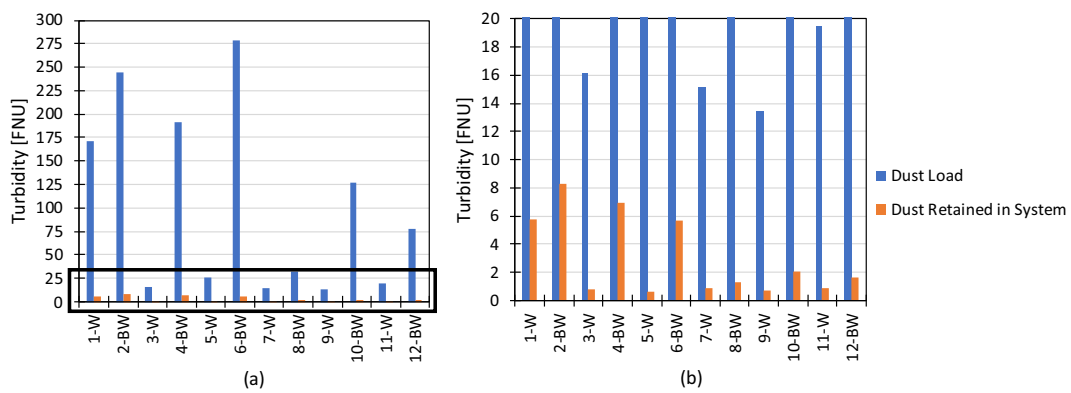

Fig. 11 **a** Dust concentrations of samples from field surfaces compared to dust concentrations of the retained dust in system using turbidity as particle concentration proxy for 12 street locations in Stockholm. **b** Magnification of the black rectangle in (**a**). W and BW stands for wheel track and between wheel track. The de-ionised water used had a reference turbidity of 0.24 FNU

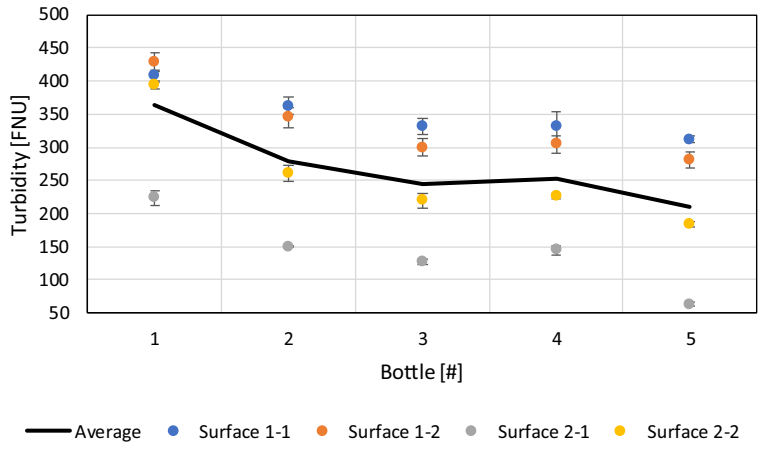

Fig. 12 Variation of dust concentration over sampling time using turbidity as proxy for two surfaces. Each turbidity value is an average of three readings. Each point corresponds roughly to 1 s of sampling. The black line corresponds to the average of all surfaces

increased amounts of water reducing the washing force against the surface. As the sample is pressed out of the sampling cylinder, the water level decreases and the washing force increases, resulting in the small increase in turbidity seen in bottle 4.

As earlier stated, this paper has only used a fixed washing time. Using a different washing time, given that other settings are constant, will likely affect the results. With the current settings, in some locations, the road dust is not fully collected due to the circumstances of the location, such as texture depth, amount of dust and degree of cementation of the dust.

6.3.4 Implications for Particle Concentration Balance

Combining the water mass balance with the implication of dust behaviour, some implications for the dust concentration of both the sample and the water losses can be discussed.

As for the water mass balance, the following assumptions are made regarding the water volumes:

$$\begin{aligned} W_{sur,k} &= W_{sur,k+1} \rightarrow V_{sur,k} = V_{sur,k+1} \\ W_{rub,k} &= W_{rub,k+1} \rightarrow V_{rub,k} = V_{rub,k+1} \\ W_{del,k} &= W_{del,k+1} \rightarrow V_{rub,k} = V_{rub,k+1} \\ \varepsilon_k &= \varepsilon_{k+1} \rightarrow V_{\varepsilon,k} = V_{\varepsilon,k+1} \end{aligned} \quad (5)$$

where V is the volume water [m^3], ε is the error and k is the notation for sample number together with other denotations described earlier, under the assumption of constant water density of 1000 kg/m^3.

Some assumptions are also made regarding the dust available on the surface, where X [g] denotes the available dust on the sampling surface, i.e. the non-cemented dust. It is also assumed that no cemented dust was sampled during the washing. Finally, it is also assumed full mixing, i.e. the dust is fully mixed in the delivered water.

Using these assumptions, the particle concentration in the first sample for a given surface area is:

$$C_{col,1} = \frac{X_{col,1}}{V_{col,1}} \leftrightarrow X_{col,1} = C_{col,1} \bullet V_{col,1} \quad (6)$$

where C is the particle concentration [kg/m^3] and X is the particle mass [kg]. It is clear from the earlier mentioned tests regarding the dust variability over time that the last second have a concentration of 74% compared to the first second of the sampling when normalised against the full sampling time. This normalisation calculation is based on the information from Fig. 12 and is presented in Table 6.

It is assumed that the concentration in remaining water on the road surface, the rubber, the container and the APN has a maximum concentration of this value (74%), possibly less than this due to the error described for the water balance. Using this assumption of maximum concentration, the particle load on the surface is calculated as:

$$\left.\begin{aligned} X_{sur,1} &= C_{sur,1} \bullet V_{sur} \\ C_{sur,1} &= 0.74 \bullet C_{col,1} \end{aligned}\right\} \rightarrow X_{sur,1} = 0.74 \bullet C_{col,1} \bullet V_{sur} \quad (7)$$

Now, for the second sample, in the same point, the mass of particles is dependent on how much water is left on the surface after sample 1, i.e. the concentration in that water, as well as on how much water is added in sample 2. Given the above assumption of full mixing and no cleaning of cemented particles, the amount of dust collected from the surface can be described as:

Table 6 Normalisation of the particle concentration for bottle of a sample, using turbidity as a proxy measurement. All bottles are approximately corresponding to 1 s of sampling. All values are related to the first bottle in the series

Surface	Turbidity related to the first bottle [%]					
	1	2	3	4	5	Average over sample
1-1	100	89	81	81	77	86
1-2	100	81	70	71	65	77
2-1	100	67	57	65	28	63
2-2	100	66	56	57	46	65
Average over surfaces	100	76	66	69	54	73*
Normalized	137	104	90	94	74	100

*Normalization is done using this value

$$X_{col,2} = X_{sur,1} \bullet \frac{V_{col,2}}{V_{del} + V_{sur}} \tag{8}$$

Since the mass of particles on the surface from sample 1 is described by Eq. 7, the following formulation is given:

$$C_{col,2} = \frac{0.74 \bullet V_{sur}}{V_{del} + V_{sur}} \bullet C_{col,1} \tag{9}$$

Using the earlier results regarding the WDS water performance, the second collected sample should then have about 3.3% of the concentration present in the first collected sample. As the earlier results present, this number is instead 6–20% for field conditions. This is possibly due either to faulty assumptions, i.e. there is no full mixing, there is cleaning of cemented particles or a combination, or that there are other losses not accounted for. It is probable that cleaning of cemented particles is the most important error sources, although this requires further investigations.

Similar equations can also be put up for the losses at the rubber sealing and due to the losses at the interface between the container and the WDS as well as the APN.

For the rubber sealing, it is reasonable to assume that it is similar to that of the surface, since the rubber sealing acts in the interface between the road surface and the WDS. A description of the amount of particles which is collected on the rubber sealing after the first sample is then:

$$X_{rub,1} = 0.74 \bullet C_{col,1} \bullet V_{rub} \tag{10}$$

For the second sample, it is reasonable to assume that the rubber sealing should behave similar to the surface, thus giving:

$$\begin{aligned} X_{rub,2} &= X_{sur,1} \bullet \frac{V_{rub}}{V_{del} + V_{sur}} \\ &= 0.74 \bullet C_{col,1} \bullet V_{sur} \bullet \frac{V_{rub}}{V_{del} + W_{sur}} \end{aligned} \tag{11}$$

which then describes the particle concentration as:

$$C_{rub,2} = \frac{X_{rub,2}}{V_{rub}} = \frac{0.74 \bullet V_{sur}}{V_{rub}} \bullet \frac{V_{rub}}{V_{del} + V_{sur}} \bullet C_{col,1} \tag{12}$$

Using this equation, the water present at the rubber sealing after the second sample will have about 3.3% of the concentration present in the first collected sample.

For the APN and the container interface, the relation is simpler, since they are not in the direct interface between the road surface and WDS as the surface and rubber sealing are. Instead, it is assumed that for the first sample, the APN:

$$C_{APN,1} = \frac{V_{APN,1}}{V_{col,1}} \bullet C_{col,1} \tag{13}$$

which then describe the concentration after the second sample as:

$$\begin{aligned} C_{APN,2} &= \frac{V_{APN,2}}{V_{col,2}} \bullet C_{col,2} \\ &= \frac{V_{APN,2}}{V_{col,2}} \bullet \frac{0.74 \bullet V_{sur}}{V_{del} + V_{sur}} \bullet C_{col,1} \end{aligned} \tag{14}$$

Using this equation, the water which leaks at the APN have a concentration of 0.5% and 0.2% for the first and second sample respectively, compared to the first collected samples concentration.

For the container interface instead, the following result is obtained for the first sample:

$$C_{con,1} = \frac{V_{con,1}}{V_{col,1}} \bullet C_{col,1} \tag{15}$$

which then describe the concentration after the second sample as:

$$C_{con,2} = \frac{V_{con,2}}{V_{col,2}} \bullet C_{col,2} = \frac{V_{con,2}}{V_{col,2}} \bullet \frac{0.74 \bullet V_{sur}}{V_{del} + V_{sur}} \bullet C_{col,1} \tag{16}$$

This gives that the leakage in the interface between the container and the WDS has a concentration of 1.4% and 3.3% respectively for the first and second sample, related to the collected first sample concentration.

As earlier determined, after the first sample, the APN has a concentration of 0.5% and the interface between container and WDS has a concentration of 1.4% compared to the collected sample concentration. After the second sample instead, it was earlier determined that the collected sample only have 3.3% of the first sample concentration, while APN has 0.2%, the interface between the container has 3.3% and the rubber also has 3.3% of the concentration, compared to the concentration of the first collected sample.

7 Conclusions and Final Remarks

This paper has described the WDS measurement system and the motives for development of a water-based sampling method. The performance of the WDS is evaluated, primarily regarding potential losses, the impact of different surfaces on the sampling performance, and the efficiency of sampling, given the used settings. The WDS performs well, with low losses of water and dust, possibly excluding the water amount left on the road surface. Within the macro texture range described, excluding the smooth concrete floor, the method shows similar losses independent of surfaces macro texture.

In a detailed study, a water mass balance was set up for repeated sampling of the same sampling surface area. Two possibilities were found: either an increased amount of water being collected for each sample, or an increased amount of water leakage at the APN and at the interface of the container and WDS.

The dust investigations using turbidity as a proxy for the concentration of dust insoluble in water showed promising results. The losses are small within the system, and likely neglectable compared to other losses, such as the potential loss on the surface based on the water loss. Both the investigation regarding dust retained on surface after first sampling, and how the dust concentration varies over the sampling time within a sample, imply that these losses are of minor importance. It is also seen in certain situations that one sample is not enough to collect all dust, which is why the measurement sequence (e.g. wash time) should be adjusted to the amount of dust, and its availability to cleaning. This should also be investigated in more detail.

A particle balance was set up, showing that, theoretically, the second sample only have 3.3% of the concentration compared to the first sample. This number is higher in field samples (6–20%), indicating that there are more aspects to consider and investigate further for a full understanding of this difference.

Despite some room for further developments and evaluations, the WDS is a versatile and repeatable sampler, also broadening the possibility to sample road dust on both wet and dry surfaces. The WDS thus fills an important role in the studies of road dust and thus the consequent understanding of air pollutants.

8 Suggested Studies and Development

To improve the method and to gain further knowledge regarding the system performance, the following studies are suggested:

- How different settings (time of washing, time of collecting, overlap of washing and collecting, pressure and water flow etc.) impact on cleaning efficiency. This should be done both in terms of the collected material and its size distributions, but also in terms of retained water on surface, leakage between sample container and sample holder.
- Investigate the impact water height or water mass present in sampling container have on losses from leakage between sample container and sample holder as well as how it affects leakage from air pressure normaliser. This is relatable to the use of smaller or larger containers, and their shape.

- Investigations on how different mass concentrations of dust and water impact on the size distributions (dry dust compared to wet), as well as how the WDS might in turn impact the size distributions further. This is also linked to determining the actual upper and lower cut-off limits, given material with a larger size than the physical limit of the system.
- Complement the current measurements with gravimetrical methods to determine actual concentrations and relate them to the turbidity proxy.
- Investigate how the size of the rubber sealing impacts on the results, e.g. how the mass sampled or retained varies with sealed surface area.

Acknowledgements The authors wish to thank and acknowledge all involved in the development and evaluation of the WDS, including OptiDrift with financiers (project about optimising street operation and maintenance to minimise road dust in Stockholm, funded by VINNOVA, the Swedish Innovation Agency), Stockholm City, the Swedish Transport Administration, The Norwegian Public Roads Administration, Nordic Envicon Oy in Finland, the Finnish Environmental Institute (SYKE), VTI workshop and measurement laboratory as well as the students and other persons involved in development and evaluation of the WDS.

Funding Information Open access funding provided by Swedish National Road and Transport Research Institute (VTI). This study was performed within a PhD program financiered by VTI and the Swedish Transport Administration.

References

Amato, F. (Ed.). (2018). *Non-exhaust emissions: an urban air quality problem for urban public health; impact and mitigation measures*. San Diego, U.S.A.: Academic Press.

Amato, F., Pandolfi, M., Alastuey, A., Lozano, A., Gonzalez, J. C., & Querol, X. (2013). Impact of traffic intensity and pavement aggregate size on road dust particles loading. *Atmospheric Environment, 77*, 711–717. https://doi.org/10.1016/j.atmosenv.2013.05.020.

Amato, F., Cassee, F. R., Denier van der Gon, H. A., Gehrig, R., Gustafsson, M., Hafner, W., et al. (2014). Urban air quality: the challenge of traffic non-exhaust emissions. *Journal of Hazardous Materials, 275*, 31–36. https://doi.org/10.1016/j.jhazmat.2014.04.053.

Blomqvist, G., Gustafsson, M., Janhäll, S., & Lundberg, T. (2014). PM10 emissions and road surface dust load is influenced by road surface macro texture. In *Nordic Society for Aerosol Research (NOSA)*.

CEN (2010). EN 13036-1 Road and airfield surface characteristics—test methods—part 1: measurement of pavement surface macrotexture depth using a volumetric patch technique. (Vol. EN 13036-1). Brusels, Belgium: European Committee for Standardization (CEN).

China, S., & James, D. E. (2012). Influence of pavement macrotexture on PM10 emissions from paved roads: a controlled study. *Atmospheric Environment, 63*, 313–326. https://doi.org/10.1016/j.atmosenv.2012.09.018.

Denby, B. R., Sundvor, I., Johansson, C., Pirjola, L., Ketzel, M., Norman, M., et al. (2013a). A coupled road dust and surface moisture model to predict non-exhaust road traffic induced particle emissions (NORTRIP). Part 2: Surface moisture and salt impact modelling. *Atmospheric Environment, 81*, 485–503. https://doi.org/10.1016/j.atmosenv.2013.09.003.

Denby, B. R., Sundvor, I., Johansson, C., Pirjola, L., Ketzel, M., Norman, M., et al. (2013b). A coupled road dust and surface moisture model to predict non-exhaust road traffic induced particle emissions (NORTRIP). Part 1: road dust loading and suspension modelling. *Atmospheric Environment, 77*, 283–300. https://doi.org/10.1016/j.atmosenv.2013.04.069.

Denier van der Gon, H. A. C., Gerlofs-Nijland, M. E., Gehrig, R., Gustafsson, M., Janssen, N., Harrison, R. M., et al. (2012). The policy relevance of wear emissions from road transport, now and in the future—an international workshop report and consensus statement. *Journal of the Air & Waste Management Association, 63*(2), 136–149. https://doi.org/10.1080/10962247.2012.741055.

EPA (1993a).AP-42, Fifth Edition, Volume I, Appendix C.1: procedures for sampling surace/bulk dust loading. U.S. Environmental Protection Agency.

EPA (1993b). AP-42, Fifth Edition, Volume I, Appendix C.2: procedures for laboratory analysis of surface/bulk dust loading samples. U.S. Environmental Protection Agency.

EPA (2011). AP-42, Fifth Edition, Volume I, Chapter 13.2.1: paved roads. U.S. Environmental Protection Agency.

Etyemezian, V., Kuhns, H., Gillies, J., Chow, J., Hendrickson, K., McGown, M., et al. (2003a). Vehicle-based road dust emission measurement (III): effect of speed, traffic volume, location, and season on PM10 road dust emissions in the Treasure Valley, ID. *Atmospheric Environment, 37*(32), 4583–4593. https://doi.org/10.1016/S1352-2310(03)00530-2.

Etyemezian, V., Kuhns, H., Gillies, J., Green, M., Pitchford, M., & Watson, J. (2003b). Vehicle-based road dust emission measurement: I—methods and calibration. *Atmospheric Environment, 37*(32), 4559–4571. https://doi.org/10.1016/S1352-2310(03)00528-4.

Etyemezian, V., Kuhns, H., Nikolich, G., Fitz, D. R., Bumiller, K., Merle, R., et al.(2005) Vehicle-based measurement of PM10 paved road dust emissions in Las Vegas, NV: Spatial distribution of emissions using TRAKER. In *Proceedings of the Air and Waste Management Association's Annual Conference and Exhibition, AWMA, Vol. 2005* .

Etyemezian, V., Kuhns, H., & Nikolich, G. (2006). Precision and repeatability of the TRAKER vehicle-based paved road dust emission measurement. *Atmospheric Environment, 40*(16), 2953–2958. https://doi.org/10.1016/j.atmosenv.2005.12.042.

Etyemezian, V., Nikolich, G., Ahonen, S., Pitchford, M., Sweeney, M., Purcell, R., et al. (2007). The Portable In Situ Wind Erosion Laboratory (PI-SWERL): a new method to measure PM10 potential for windblown dust properties and emissions. *Atmospheric Environment, 41*(18), 3789–3796. https://doi.org/10.1016/j.atmosenv.2007.01.018.

Forsberg, B., Hansson, H. C., Johansson, C., Areskoug, H., Persson, K., & Jarvholm, B. (2005). Comparative health impact assessment of local and regional particulate air pollutants in Scandinavia. *Ambio, 34*(1), 11–19.

Grayson, R. B., Finlayson, B. L., Gippel, C. J., & Hart, B. T. (1996). The potential of field turbidity measurements for the computation of total phosphorus and suspended solids loads. *Journal of Environmental Management, 47*(3), 257–267. https://doi.org/10.1006/jema.1996.0051.

Grigoratos, T., & Martini, G. (2015). Brake wear particle emissions: a review. *Environmental Science and Pollution Reseach International, 22*(4), 2491–2504. https://doi.org/10.1007/s11356-014-3696-8.

Gustafsson, M., Blomqvist, G., Gudmundsson, A., Dahl, A., Swietlicki, E., Boghard, M., Lindbom, J., & Ljungman, A. (2008). Properties and toxicological effects of particles from the interaction between tyres, road pavement and winter traction material. *Science of the Total Environment, 393*, 226–240. https://doi.org/10.1016/j.scitotenv.2007.12.030.

Gustafsson, M., Blomqvist, G., Gudmundsson, A., Dahl, A., Jonsson, P., & Swietlicki, E. (2009). Factors influencing PM_{10} emissions from road pavement wear. *Atmospheric Environment, 43*(31), 4699–4702. https://doi.org/10.1016/j.atmosenv.2008.04.028.

Gustafsson, M., Blomqvist, G., Jonsson, P., & Ferm, M. (2010). Effekter av dammbindning av belagda vägar. *VTI Rapport 666*. Linköping: Statens väg- och transportforskningsinstitut (VTI). [In Swedish].

Gustafsson, M., Bennet, C., Blomqvist, G., Johansson, C., Norman, M., & Sjövall, B. (2011). Utvärdering av städmaskiners förmåga att minska PM10-halter. *VTI Rapport 707*. Linköping: Statens väg- och transportforskningsinstitut (VTI). [In Swedish].

Gustafsson, M., Blomqvist, G., Janhäll, S., Johansson, C., & Norman, M. (2014b). Driftåtgärder mot PM10 i Stockholm : utvärdering av vintersäsongen 2012–2013. VTI Rapport 802. Linköping: VTI. [In Swedish].

Gustafsson, M., Blomqvist, G., Johansson, C., & Norman, M. (2013). Driftåtgärder mot PM10 på Hornsgatan och Sveavägen i Stockholm - utvärdering av vintersäsongen 2011-2012. *VTI-Rapport 767*. Linköping: Statens väg- och transportforskningsinstitut (VTI). [In Swedish].

Gustafsson, M., Forsberg, B., Orru, H., Åström, S., Tekie, H., & Sjöberg, K. (2014). Quantification of population exposure to NO_2, $PM_{2.5}$ and PM_{10} and estimated health impacts in Sweden 2010. Stockholm, Sweden: IVL Swedish Environmental Research Institute.

Gustafsson, M., Blomqvist, G., Janhäll, S., Johansson, C., & Norman, M. (2015). Driftåtgärder mot PM10 i Stockholm : utvärdering av vintersäsongen 2013–2014. *VTI Rapport 847*. Linköping: Statens väg- och transportforskningsinstitut (VTI). [In Swedish].

Gustafsson, M., Blomqvist, G., Janhäll, S., Norman, M., & Johansson, C. (2016). Driftåtgärder mot PM10 i Stockholm : utvärdering av vintersäsongen 2014–2015. *VTI Rapport 897*. Linköping: Statens väg- och transportforskningsinstitut (VTI). [In Swedish].

Gustafsson, M., Blomqvist, G., Janhäll, S., Johansson, C., Järlskog, I., Lundberg, J., et al. (2017). Driftåtgärder mot PM10 i Stockholm : utvärdering av vintersäsongen 2015–2016. *VTI rapport 928*. Linköping: Statens väg- och transportforskningsinstitut (VTI). [In Swedish].

Gustafsson, M., Blomqvist, G., Järlskog, I., Lundberg, J., Janhäll, S., Elmgren, M., et al. (2019). Road dust load dynamics and influencing factors for six winter seasons in Stockholm, Sweden. *Atmospheric Environment: X, 2*, 100014. https://doi.org/10.1016/j.aeaoa.2019.100014.

Harrison, R. M., Jones, A. M., Gietl, J., Yin, J., & Green, D. C. (2012). Estimation of the contributions of brake dust, tire wear, and resuspension to nonexhaust traffic particles derived from atmospheric measurements. *Environmental Science & Technology, 46*(12), 6523–6529. https://doi.org/10.1021/es300894r.

Hetem, I., & Andrade, M. (2016). Characterization of fine particulate matter emitted from the resuspension of road and pavement dust in the metropolitan area of São Paulo, Brazil. *Atmosphere, 7*(3), 31.

ISO 13473-1 (1997). Characterization of pavement texture by use of surface profiles—part 1: determination of mean profile depth. (Vol. 13473–1). Genève, Switzerland: International Organization for Standardization (ISO).

Janhäll, S., Gustafsson, M., Andersson, K., Järlskog, I., & Lindström, T. (2016). Utvärdering av städmaskiners förmåga att reducera vägdammsförrådet i gatu- och tunnelmiljöer i Trondheim. *VTI rapport 883*. Linköping: Statens väg- och transportforskningsinstitut (VTI). [In Swedish].

Järlskog, I., Blomqvist, G., Gustafsson, M., & Janhäll, S. (2017). Utvärdering av städmaskiners förmåga att reducera vägdammsförrådet i gatu- och tunnelmiljöer : En fältstudie i Trondheim 2016. VTI rapport 953. Linköping: Statens väg- och transportforskningsinstitut. [In Swedish].

Jonsson, P., Blomqvist, G., & Gustafsson, M. (2008). Wet dust sampler: Technological innovation for sampling particles and salt on road surface. *Seventh International Symposium on Snow Removal and Ice Control Technology, Transportation Research Circular, E-C126*, 102-111.

Kauhaniemi, M., Stojiljkovic, A., Pirjola, L., Karppinen, A., Harkonen, J., Kupiainen, K., et al. (2014). Comparison of the predictions of two road dust emission models with the measurements of a mobile van. *Atmospheric Chemistry and Physics, 14*(17), 9155–9169. https://doi.org/10.5194/acp-14-9155-2014.

Kuhns, H., Etyemezian, V., Landwehr, D., MacDougall, C., Pitchford, M., & Green, M. (2001). Testing re-entrained aerosol kinetic emissions from roads (TRAKER): a new approach to infer silt loading on roadways. *Atmospheric Environment, 35*(16), 2815–2825. https://doi.org/10.1016/S1352-2310(01)00079-6.

Lanzinger, S., Schneider, A., Breitner, S., Stafoggia, M., Erzen, I., Dostal, M., et al. (2016). Associations between ultrafine and fine particles and mortality in five central European cities—results from the UFIREG study. *Environment International, 88*, 44–52. https://doi.org/10.1016/j.envint.2015.12.006.

Lundberg, J., Blomqvist, G., Gustafsson, M., & Janhäll, S. (2017). Texture influence on road dust load. Paper presented at the Transport and Air Pollution, Zürich, Switzerland.

Meister, K., Johansson, C., & Forsberg, B. (2012). Estimated short-term effects of coarse particles on daily mortality in Stockholm, Sweden. *Environmental Health Perspectives, 120*(3), 431–436. https://doi.org/10.1289/ehp.1103995.

Padoan, E., Ajmone-Marsan, F., Querol, X., & Amato, F. (2018). An empirical model to predict road dust emissions based on pavement and traffic characteristics. *Environmental Pollution, 237*, 713–720. https://doi.org/10.1016/j.envpol.2017.10.115.

Pavanelli, D., & Bigi, A. (2005). Indirect methods to estimate suspended sediment concentration: reliability and relationship of turbidity and settleable solids. *Biosystems Engineering, 90*(1), 75–83. https://doi.org/10.1016/j.biosystemseng.2004.09.001.

Pirjola, L., Parviainen, H., Hussein, T., Valli, A., Hameri, K., Aaalto, P., et al. (2004). "Sniffer"—a novel tool for chasing vehicles and measuring traffic pollutants. *Atmospheric Environment, 38*(22), 3625–3635. https://doi.org/10.1016/j.atmosenv.2004.03.047.

Pirjola, L., Kupiainen, K. J., Perhoniemi, P., Tervahattu, H., & Vesala, H. (2009). Non-exhaust emission measurement system of the mobile laboratory SNIFFER. *Atmospheric Environment, 43*(31), 4703–4713. https://doi.org/10.1016/j.atmosenv.2008.08.024.

Pirjola, L., Johansson, C., Kupiainen, K., Stojiljkovic, A., Karlsson, H., & Hussein, T. (2010). Road dust emissions from paved roads measured using different mobile systems. *Journal of the Air & Waste Management Association, 60*(12), 1422–1433. https://doi.org/10.3155/1047-3289.60.12.1422.

Shaughnessy, W. J., Venigalla, M. M., & Trump, D. (2015). Health effects of ambient levels of respirable particulate matter (PM) on healthy, young-adult population. *Atmospheric Environment, 123*, 102–111. https://doi.org/10.1016/j.atmosenv.2015.10.039.

Slaets, J. I. F., Schmitter, P., Hilger, T., Lamers, M., Piepho, H. P., Vien, T. D., et al. (2014). A turbidity-based method to continuously monitor sediment, carbon and nitrogen flows in mountainous watersheds. *Journal of Hydrology, 513*, 45–57. https://doi.org/10.1016/j.jhydro1.2014.03.034.

Stafoggia, M., Samoli, E., Alessandrini, E., Cadum, E., Ostro, B., Berti, G., et al. (2013). Short-term associations between fine and coarse particulate matter and hospitalizations in Southern Europe: results from the MED-PARTICLES project. *Environmental Health Perspectives, 121*(9), 1026–1033. https://doi.org/10.1289/ehp.1206151.

Tananaev, N. I., & Debolskiy, M. V. (2014). Turbidity observations in sediment flux studies: examples from Russian rivers in cold environments. *Geomorphology, 218*, 63–71. https://doi.org/10.1016/j.geomorph.2013.09.031.

Thorpe, A., & Harrison, R. M. (2008). Sources and properties of non-exhaust particulate matter from road traffic: a review. *Science of the Total Environment, 400*(1–3), 270–282. https://doi.org/10.1016/j.scitotenv.2008.06.007.

Wehrens, R., Putter, H., & Buydens, L. M. C. (2000). The bootstrap: a tutorial. *Chemometrics and Intelligent Laboratory Systems, 54*(1), 35–52. https://doi.org/10.1016/S0169-7439(00)00102-7.

WHO Regional Office for Europe OECD. (2015). *Economic cost of the health impact of air pollution in Europe: clean air, health and wealth*. Copenhagen: WHO Regional Office for Europe.